

## Chapter 3

### Bulk and surface contributions to resonant SHG

#### 3.1 Introduction

Surface SHG has proven to be a powerful diagnostic technique for studying the properties of buried Si-SiO<sub>2</sub> interfaces [29, 54], which are important to semiconductor technology. It has been shown that SHG is very sensitive to medium surface conditions, such as crystal orientation [24], miscut [55, 56], and roughness [56-58]. It is also well known that SHG is sensitive to laser parameters, such as polarization and wavelength [33, 59]. Thus, care must be taken when interpreting results or inter-comparing published results.

The SHG signal from Si(001) consists of a strong electric-dipole allowed contribution from the surface (or interface) and a weaker one due to the electric-quadrupole and magnetic-dipole terms in the bulk [60] (also see Chapter 2). The expectation that the bulk contribution is relatively independent of surface conditions suggests that it can be used as a reference to aid in comparison between samples, as has been done in studying the effect of interface roughness [56-58]. However, by combining spectroscopic and rotational-anisotropy SHG (RA-SHG) measurements, we have discovered that the bulk contribution displays resonant behavior. This was not reported in earlier spectroscopic studies of SHG from oxidized [33, 59] or hydrogen terminated [61] silicon. The resonant behavior must be accounted for if the bulk contribution is used as a reference to compare samples. Furthermore, the bulk

contribution can interfere with the surface contribution, thereby shifting the apparent resonance position for data taken at a single azimuthal angle [33, 59].

The SHG response is described by nonlinear optical susceptibility tensors that connect the generated signal to the electric field of the incident beam, as shown in Chapter 2. Ideally, it would be possible to completely measure all of the tensor elements of the susceptibility tensors that describe the bulk and surface contributions. For spectroscopic measurements, the variation of the tensor elements as function of the photon energy of the emitted (or incident) light would be measured. However, it is fundamentally difficult to separate the isotropic bulk and surface contributions [28]. Nevertheless, by careful use of RA-SHG in combination with polarization selective SHG, we are able to provide some separation of the tensor elements, which improves comparison among samples. While full phase information can be obtained by dispersion detection with a reference [62] or by homodyne detection with a reference [63], we can obtain relative phase information from our simpler experiment. We observe that the isotropic response, which includes contribution from both surface and bulk, displays a resonance that is sensitive to surface preparation. The two photon resonant energy is 3.39 eV for native oxide silicon (NO-Si), while it shifts to 3.35 eV for a thermal oxide (TO-Si) sample. The anisotropic component, which in a simple picture is only due to the bulk, has a resonance at 3.42 eV, for NO-Si, TO-Si, and hydrogen terminated Si (H-Si). Prior work observed resonances around 3.3 eV and ascribed them to the  $E_1$  critical point (CP) due to the band structure of bulk silicon with a red shift due to sub-interface strain of the Si-Si bonds by the oxide layer [33]. Based on studying the effect of surface modification, this earlier work concluded that

the resonance was purely in the surface contribution and not due to the bulk contribution. This is contrary to our conclusions based on RA-SHG; however, we can explain this difference as arising from interfering surface and bulk contributions that can distort the spectroscopic results taken for a single azimuthal angle.

### 3.2 Bulk and surface SHG contributions

In bulk crystalline Si, SHG arises only from the nonlocal response characterized by two phenomenological constants  $\zeta$  and  $\gamma$ , which are anisotropic and isotropic respectively [27]. SHG from a (001) surface or interface is isotropic. These symmetry properties are systematically presented in Chapter 2. With the polarizations limited to  $s$  and  $p$  states, we write the total SH fields  $E_{g,h}^{(2\omega)}$  from a Si(001) crystal face as

$$E_{g,p}^{(2\omega)}(\phi) = [a_{0,(g,p)} e^{i\theta_{g,p}} + a_{4,(g,p)} \cos(4\phi)] e^{i\delta_{g,p}} E_g^2, \quad (3.1)$$

$$E_{g,s}^{(2\omega)}(\phi) = a_{4,(g,s)} \sin(4\phi) e^{i\delta_{g,s}} E_g^2. \quad (3.2)$$

Here,  $E_g$  is the incident fundamental field, and  $\phi$  is the azimuthal angle between the incident plane and [100] direction in the sample surface plane. The notation  $(g, h)$  represents  $g$  polarized fundamental and  $h$  polarized harmonic radiation, where  $g$  and  $h = s$  or  $p$ . The SHG intensity  $I_{g,h}^{(2\omega)}(\phi)$  is proportional to the magnitude square of the SH field, i.e.,  $I_{g,h}^{(2\omega)}(\phi) \propto |E_{g,h}^{(2\omega)}(\phi)|^2$ . Both  $\theta$  and  $\delta$  provide phase information, but  $\delta$  is irrelevant when only the intensity is measured. The constants  $a_0$  and  $a_4$  are the magnitudes of the isotropic and anisotropic contributions to the RA-SHG signal, respectively. They are determined by the relevant susceptibility elements, Fresnel

factors, and dielectric functions. The dependence of  $a_4$  on the laser frequency,  $\omega$ , involves only  $\zeta$  and two dielectric functions  $\varepsilon(\omega)$  and  $\varepsilon(2\omega)$ , as shown in Chapter 2. It can be written as

$$a_{4,(g,h)}(\omega) = f_{(g,h)}(\zeta(\omega), \varepsilon(\omega), \varepsilon(2\omega)) = L_{(g,h)}(\omega) |\zeta(\omega)|, \quad (3.3)$$

where  $L_{(g,h)}(\omega)$  is a function of frequency arising from linear optics. The polarization dependence in  $a_4$  and  $L$  results from the geometry of experiment.

### 3.3 Sample preparation and experimental method

The samples were prepared from the same undoped ( $\rho > 20 \Omega \cdot \text{cm}$ ), on-axis Si(001) wafer. The NO-Si sample, covered with 2 nm thick native oxide, was investigated as received from the manufacturer. The TO-Si sample was prepared by oxidation of chemically cleaned NO-Si at 1000 °C in a dry oxygen atmosphere to yield an oxide of 14 nm thickness. Before the thermal oxidation process, natively oxidized Si wafers were cleaned followed the standard the RCA cleaning process [64]. Two H-Si samples were obtained by dipping NO-Si and TO-Si samples in an  $\text{NH}_4\text{F}:\text{HF}$  buffered oxide etch (BOE). The durations of the BOE were controlled, so that oxides were just removed but the samples were not over-etched [65]. The difference in the SH signals from these two H-terminated samples are negligible, so we do not distinguish between them.

The experimental setup is described in detail in Chapter 1. We used a modelocked laser with ~150 fs pulse width, 76 MHz repetition rate, and wavelength tunable from 700 to 810 nm. The ~60 mW beam was focused to <30  $\mu\text{m}$  on the samples at 45° incident angle. During the experiment, the samples were held in a

chamber purged by dry  $N_2$  to reduce the charging effect [66] and oxidation of the H-Si samples. The SHG signals in reflection were detected by photomultiplier tubes with 1 sec gate time. The SHG spectra were calibrated against the SHG signal in reflection from a quartz sample. The uncertainty at each point is estimated by taking multiple scans and calculating the standard deviation at each point. These uncertainty estimates are then used in the fitting procedure to estimate the uncertainty of the fit coefficients. The uncertainty in the photon energy is due to the laser bandwidth, which was measured at each wavelength and varies between 20 and 30 meV (two-photon energy). Error bars are omitted in the figures if they are smaller than the plot symbol.

### 3.4 Experimental results

#### 3.4.1 Spectroscopic results of the bulk anisotropic contribution

To separate out the bulk anisotropic contribution, we use a combination of polarization and RA-SHG. For Si(001) surfaces, the anisotropic coefficient,  $a_4$ , is only due to the bulk while the isotropic coefficient,  $a_0$ , is mainly due to the surface, but includes a weak bulk contribution. To provide a clean measurement of the bulk anisotropic contribution, we measured RA-SHG in the  $(p, s)$  configuration as a function of photon energy. The spectra obtained this way showed negligible dependence on surface modification. The spectrum of  $a_{4,(p,s)}$  for NO-Si is shown in Fig. 3.1, which shows a peak at 3.42 eV two-photon energy. Using Eq. (3.3), we can obtain a spectrum for  $\zeta(\omega)$ . The function  $L_{(p,s)}(\omega)$  is calculated using the phenomenological theory in Chapter 2 and tabulated values for the dielectric

functions of crystalline silicon [67].  $L_{(p,s)}(\omega)$  displays a weak minimum around 3.35 eV, which shifts the resonance of  $\zeta(\omega)$  compared to that of  $a_{4,(p,s)}$ , yielding a peak at 3.38 eV for  $\zeta(\omega)$  as shown in Fig. 3.1. This resonance energy is between the  $E_0'$  CP energy of 3.33 eV and  $E_1$  CP energy of 3.42 eV [68], which suggests contributions from both critical points. We note that the data in Fig. 3.1 are normalized so that  $a_{4,(s,s)}(3.26 \text{ eV}) = 1$  by using Eq. (3.3), i.e., the appropriate ratios of  $L_{(g,h)}$ . All peak positions have an uncertainty of  $\pm 0.01$  eV due to the laser bandwidth in the vicinity of the peaks.

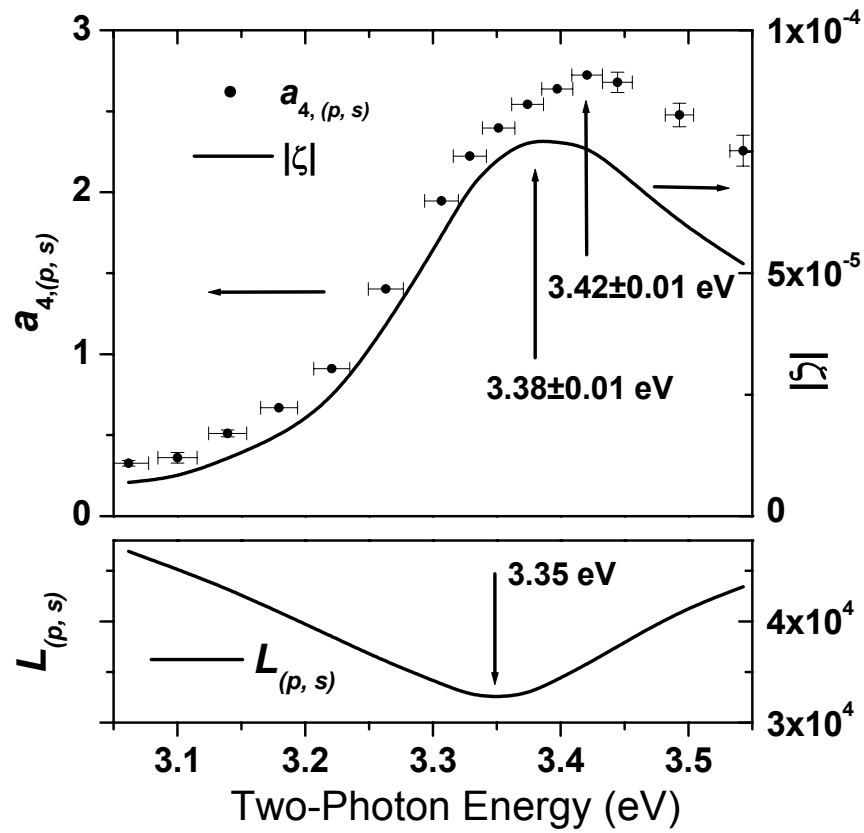


Fig. 3.1. Spectra of the anisotropic SHG contribution  $a_{4,(p,s)}$  (normalized to  $a_{4,(s,s)}$  at 3.26 eV), the linear optics coefficient  $L_{(p,s)}$  and the magnitude ( $|\zeta|$ ) of the anisotropic element  $\zeta$ . The normalization of  $a_{4,(p,s)}$  determines the magnitude of  $|\zeta|$ . The vertical error bars come from data fitting and the horizontal error bars come from the laser bandwidth.

### 3.4.2 Spectroscopic results of the isotropic contribution

Based on this measurement of the spectrum of the anisotropic bulk component from  $a_{4,(p,s)}$ , we obtain the spectrum of  $a_{4,(p,p)}$  by using the calculated spectrum of  $L_{(p,s)}$  and  $L_{(p,p)}$ . Combined with measured  $(p, p)$  polarized RA-SHG spectrum, this allows us to accurately determine both the amplitude and relative phase of the isotropic component, which includes an inseparable combination of bulk and surface contributions. Previous spectral measurements have not used a combination of  $(p, s)$  and  $(p, p)$  measurements but rather only the latter [69, 70]. However, we find the fits to the RA-SHG data are not robust when only  $(p, p)$  data are used, resulting in a large uncertainty in the fit coefficients. Typical RA-SHG data at a two-photon energy of 3.26 eV (fundamental wavelength of 760 nm) for all three samples are shown in Fig. 3.2. Clearly the azimuthal dependence of the RA-SHG signal for H-Si displays a phase shift with respect to the other two signals. This is indicative of a phase shift of the isotropic response with respect to the anisotropic bulk response, which is confirmed by our analysis. Based on complex phasor notation, we designate the quadrature components of the isotropic response with respect to the anisotropic bulk response as  $a_{0,r}$  and  $a_{0,i}$ , i.e.,  $a_{0,r} + ia_{0,i} = a_{0,(g,p)}e^{i\theta_{g,p}}$  in Eq. (3.1). This conveniently breaks the isotropic response into interfering ( $a_{0,r}$ ) and non-interfering ( $a_{0,i}$ ) components. Note that there is an ambiguity in sign of  $a_{0,i}$  obtained from our analysis.

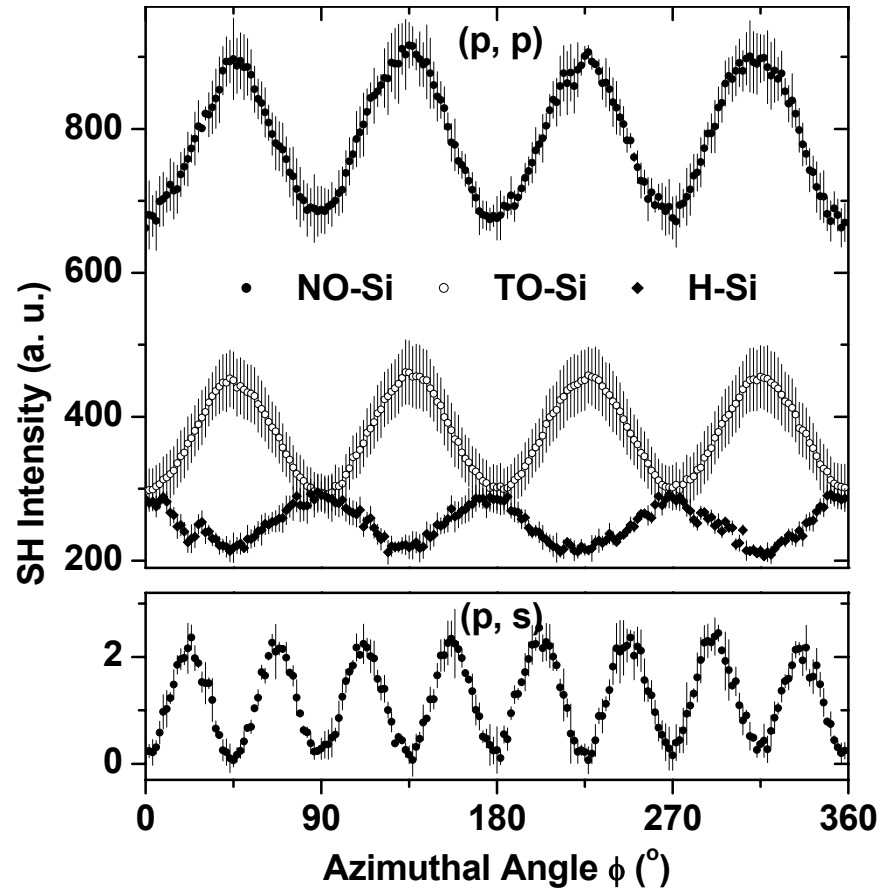


Fig. 3.2. RA-SHG intensities from modified Si(001) surfaces (NO-Si, TO-Si and H-Si) at a two-photon energy of 3.26 eV for different polarization configurations:  $(p, p)$ , top panel and  $(p, s)$ , bottom panel. The error bars are the standard deviation obtained from averaging successive scans.

The spectra of  $a_{0,r}$  (for NO-Si and TO-Si),  $a_{0,r}$  and  $a_{0,i}$  (for H-Si) are shown in Fig. 3.3. The measurements show that for NO-Si and TO-Si  $\theta \sim \pi$ , thus  $a_{0,i}$  is negligible and  $a_{0,r} < 0$  (we actually plotted  $-a_{0,r}$ ). The  $a_{0,r}$  for NO-Si peaks at two-photon energy of 3.39 eV, while for TO-Si, it peaks at 3.35 eV. Both of these show a shift to lower energy as compared to the bulk resonance, with a larger shift for the thicker oxide. The shift direction is consistent with previous results [33, 59]. As expected from the phase shift in Fig. 3.2,  $a_{0,r}$  for H-Si is opposite sign ( $> 0$ ) as compared to the oxide samples. In addition, the non-interfering quadrature,  $a_{0,i}$ , is comparable in magnitude to  $a_{0,r}$  for H-Si although their relative strength varies with photon energy.

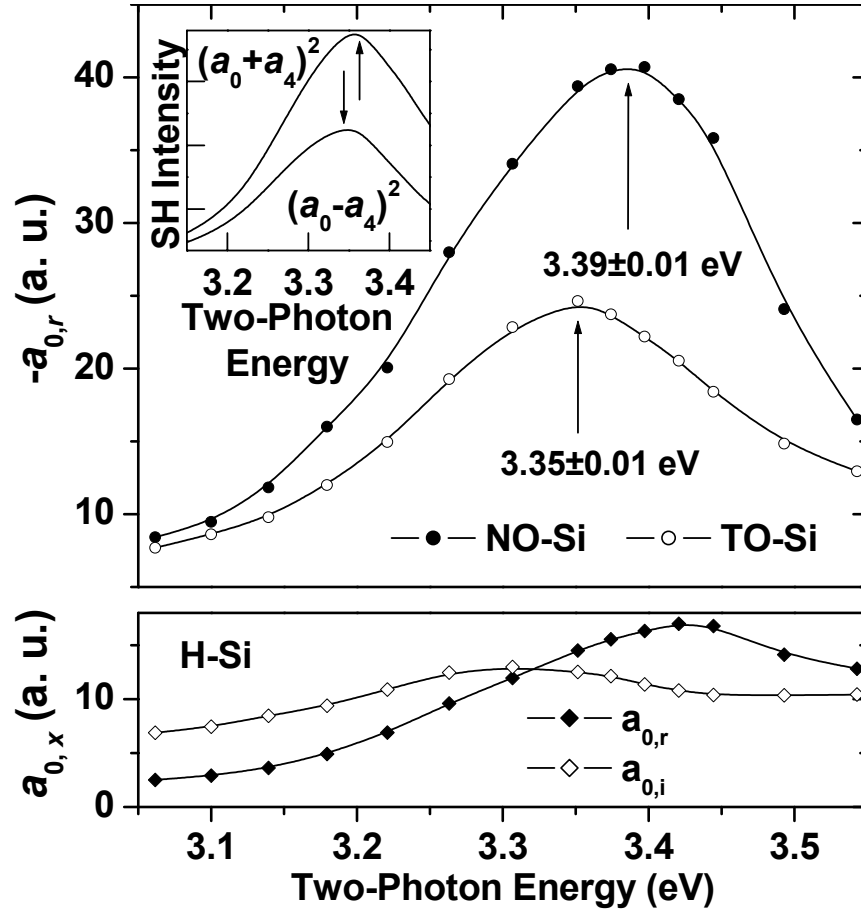


Fig. 3.3. Spectra of the isotropic amplitudes  $a_{0,r}$  for NO-Si and TO-Si (top panel) and the interfering and non-interfering isotropic amplitudes  $a_{0,r}$  and  $a_{0,i}$  for H-Si (bottom panel). The inset in the top panel shows the resonance energy shift due to interference between  $a_0$  and  $a_4$  for TO-Si for fixed azimuthal angles of  $0^\circ$  ( $a_0 - a_4$ ) and  $45^\circ$  ( $a_0 + a_4$ ). The uncertainties in energy are the same as Fig. 3.1.

### 3.5 Discussion

The stronger signal for the NO-Si, as compared to the TO-Si, is in part due to an induced electric field across the Si-SiO<sub>2</sub> interface [66]. This occurs because photo-excited electrons become trapped in the oxide or at the interface, yielding a time-dependent enhancement of the signal. In the NO-Si sample, this enhancement happens within a few seconds, and thus can cause a significant enhancement within the 1 second gate time of the photon-counting electronics. In the TO-Si sample, the enhancement takes tens of seconds to occur and thus is weak within the 1 sec gate time (the rotation brings a new portion of the sample into the focal spot for each measurement). It is important to note that the enhancement itself also displays resonant behavior, which further complicates interpretation of the spectrum obtained for a sample with a thin oxide. The original work on this time-dependent increase observed that it is enhanced when oxygen was present in the ambient [66]. Based on this, we used a nitrogen purge to try to reduce the effect, but nevertheless observe a strong time-dependent signal on resonance. This suggests that additional processes may contribute to the time-dependent enhancement for on-resonance excitation.

The remarkable phase difference of the SHG signal from the H-Si sample, compared to the oxidized samples, is indicative of the different properties of the hydrogen terminated surface compared to an oxidized surface. An ideal truncated Si surface would be electrically neutral; however the electronic structure is modified by the presence of hydrogen or oxygen, which have differing electronegativity. The peak of the signal for H-Si sample is very close to that of the bulk anisotropic response, consistent with a lack of the strain present in the oxidized samples.

The interference between the bulk anisotropic term and the isotropic terms can cause a shift in the apparent resonance position of the SHG signal if spectral data are only taken at a single azimuthal angle, as has been done in some experiments [33, 59]. This arises because of the shift between the bulk resonance and the surface resonance. As illustrated in the inset to Fig. 3.3, the peak position for the net resonance depends on whether the interference is constructive or destructive. Although a small shift, it can be comparable to the shifts due to sample preparation. Furthermore, the  $\pi$  phase shift of  $a_{0,r}$  between oxidized silicon and H-Si may lead to misleading conclusions about the relative strength of the SHG signals for data taken at a fixed angle.

### 3.6 Summary

We have used a careful combination of rotational anisotropy SHG and polarization dependent SHG from Si(001) samples to separate anisotropic bulk terms from isotropic terms, which are dominated by the surface. This shows that the bulk response does display a resonance. Using this information, we are then able to identify the amplitude and phase of the isotropic terms. A bulk anisotropic resonance is observed at a two-photon energy of 3.42 eV, which results from the interaction of the bulk susceptibility tensor element  $\zeta$  (peak at 3.38 eV) and linear optical propagation factors. The isotropic surface contributions for native oxide Si and thermal oxide Si show peaks at 3.39 eV and 3.35 eV, respectively. Interference between these contributions and the bulk signal can shift the apparent resonance position if they are not separated. Oxidation clearly induces a red shift of the resonance relative to the bulk, which is ascribed to interface strain induced by the

oxide layer. For the  $(p, p)$  polarization, oxidized surfaces only produce a signal that interferes with the anisotropic bulk signal, whereas H-Si produces both interfering and non-interfering (in-quadrature) signals. Furthermore, there is a phase shift between the interfering terms for oxidized Si as compared to H-Si. These effects can modify the apparent spectrum obtained for a fixed azimuthal angle.